Constrained large angle reorientation manoeuvres of a space telescope using potential functions and a variable control gain

G. Mengali
g.mengali@ing.unipi.it
A. A. Quarta
a.quarta@ing.unipi.it
University of Pisa
Pisa, Italy

NOMENCLATURE

E	quaternions matrix, see Equation (9)
k	dimensionless control parameter
i, j, k	body reference frame unit vectors
I	principal moment of inertia
I	inertia matrix
M	control torque
n	unit vector
q_i	quaternion (with $i = 0, 1, 2, 3$)
O	spacecraft's centre-of-mass
T	transformation matrix, see Equation (5)
$\mathcal{T}_B(x,y,z)$	body reference frame
$\mathcal{T}_I(X,Y,Z)$	inertial reference frame

Paper No. 3870. Manuscript received 2 July 2012, revised version received 10 October 2012
2nd revised version received, accepted 15 March 2013.
https://doi.org/10.1017/S0001924000008460 Published online by Cambridge University Press

t	time
V	artificial potential
δ	slew angle
γ	solar array sun angle, see Equation (2)
η	dimensionless control parameter
$\boldsymbol{\omega}$	spacecraft's angular velocity ($\omega = \|\|\boldsymbol{\omega}\|\|$)
Ω	angular velocity matrix, see Equation (8)

Subscripts

0	initial
$\oplus$	Earth
δ	depending on attitude
ω	depending on angular velocity
f	final, desired
$\odot$	Jupiter
$\mathbb{C}$	Moon
P	scientific payload
$\odot$	Sun
SA	solar array
$\star$	target
th	threshold

Superscripts

h	high value
l	low value
.	time derivative
max	maximum
$\wedge$	forbidden cone's aperture angle

1.0 INTRODUCTION

In some space applications, such as satellite surveillance and communication, a spacecraft must perform accurate pointing and slewing manoeuvres, whereby the spacecraft is rotated along a large angle amplitude trajectory. In many circumstances it is also required that the sensitive payload does not intercept bright objects such as the Sun, Earth and Moon, to avoid possible damage to the optical instruments. The importance of this subject has stimulated an active research, and different approaches have been reported in the literature[1-5].

The ways in which these manoeuvres are performed are important and, indeed, a natural choice is to deal with the reorientation problem within a time-optimal framework. In particular, the unconstrained problem has been addressed from different viewpoints [6-7], including the combined case of time and propellant optimisation[8]. Time-optimal spacecraft slewing manoeuvres with path constraints are much more difficult to synthesise. As a matter of fact, inclusion of path constraints requires augmenting the Hamiltonian function with additional terms describing those constraints[9]. Even though the resulting problem can, in principle, be tackled using an indirect approach, the path constraints create particularly difficult challenges. For these reasons Melton[10,11] has recently proposed resorting to direct methods, which offer the theoretical advantage of easier

https://doi.org/10.1017/S0001924000008460 Published online by Cambridge University Press

problem management. However, it is known that an optimal solution of a spacecraft reorientation manoeuvre, or even a feasible solution, cannot be automatically guaranteed[10]. Therefore, often the optimality of a manoeuvre may be of lesser importance than the capability of actually generating a feasible trajectory using modest computational efforts and simple implementation.

From this viewpoint an interesting option is offered by potential function based methods. These are inspired by robotics control and have been proposed to simplify frequent reorientation manoeuvres of spacecraft with autonomous re-targeting capabilities[12-16]. An interesting feature of potential function methods is that the control torques are evaluated in closed form, thus facilitating the on-board implementation with reduced software requirements and clear advantages over other available control systems. However, some limitations have been pointed out that could hinder their practical use. For instance, Ref. 17 emphasised a possible intrinsic disadvantage of potential methods due to the fact that the spacecraft, while avoiding the forbidden directions, moves substantially away from its nominal path. The aim of this paper is to show that the above drawbacks can be circumvented with a suitable choice of both the potential function and the control law. To better explain these points, it is useful to briefly summarise the potential function approach.

Basically, a scalar nonnegative (artificial) potential function is defined so that it has a global minimum at the desired final attitude, and has regions of high potential corresponding to the forbidden directions. The spacecraft controls are then chosen in such a way that the rate of change of the potential is negative. According to the Lyapunov's direct method, this guarantees that the spacecraft dynamics converges towards the desired direction. To simplify the control system design it has been suggested[12-14] that the potential gradient be made proportional to the spacecraft kinetic energy through a constant control gain k. In other terms, the artificial potential function may be formulated by including appropriate terms involving the measured angular velocity components. This is possible because the choice of the artificial potential function is not unique.

Unfortunately, good reorientation capabilities are conflicting with such a simple control law. Indeed, loosely speaking, high values of the control gain correspond to a slow spacecraft movement, whereas small values of k correspond to rapid reorientation manoeuvres. Of course, due to saturation problems, the spacecraft cannot be accelerated up to an arbitrarily high rotational velocity, otherwise the control torques would not be able to slow down the vehicle when it passes near an obstacle or approaches the pointing direction. On the other hand, too high gain values would provide unacceptably long time responses.

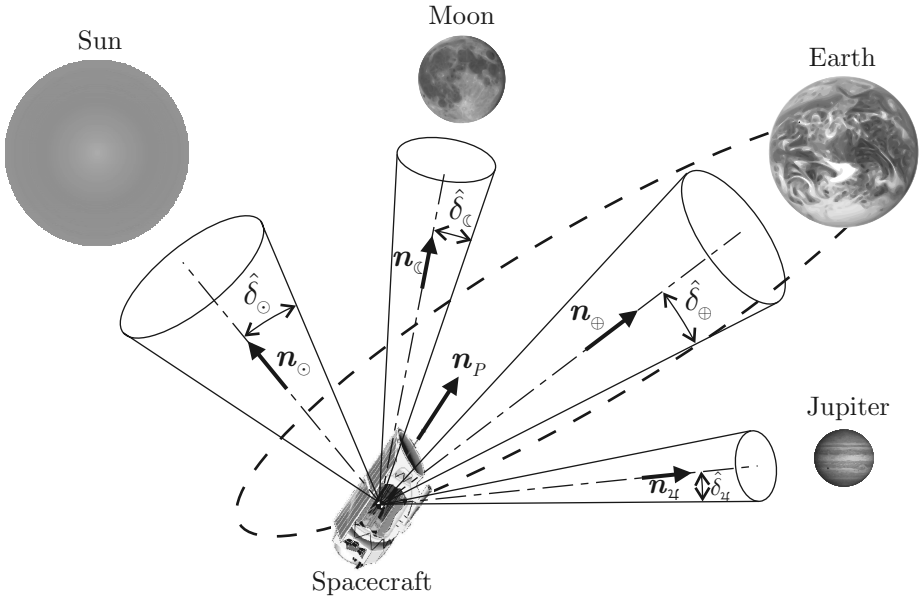
The contribution of this paper is to show that a good compromise solution is a time variant control gain whose value depends both on the spacecraft kinetic energy and on the distance from the forbidden directions. The new control law is based on simple physical considerations and permits the spacecraft to reach points in the potential field arbitrarily close to a constraint and to manoeuvre with autonomous capability of guidance and control.

2.0 PROBLEM DESCRIPTION

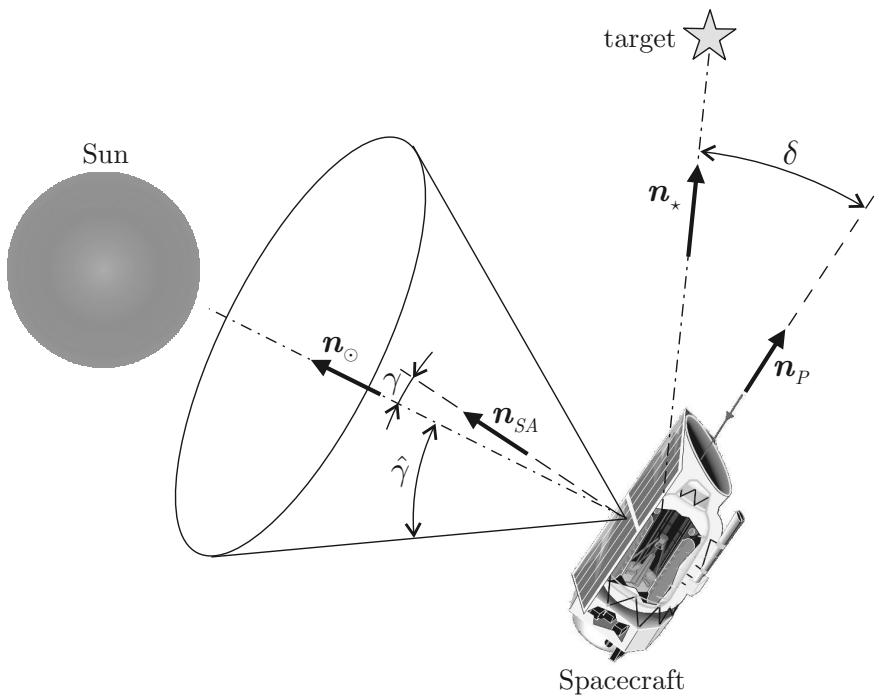
Assume that a spacecraft must perform a reorientation manoeuvre characterised by a payload pointing direction with respect to an inertial reference frame $T_I(X,Y,Z)$. During such a manoeuvre the spacecraft must avoid different pointing constraints and, at the same time, guarantee a minimum angle between the solar array nominal plane and the Sun-spacecraft direction[16], see Fig. 1.

For mathematical convenience a payload unit vector $\mathbf{n}_P$ and a solar array unit vector $\mathbf{n}_{SA}$ are now introduced. Both unit vectors are fixed with respect to the spacecraft's main body. The pointing constraints are specified in terms of $m \geq 1$ forbidden directions with respect to the inertial frame and serve to avoid that the scientific payload is damaged by bright sky regions, due to the Sun

https://doi.org/10.1017/S0001924000008460 Published online by Cambridge University Press



(a) Forbidden cones



(b) Solar array pointing requirement

Figure 1. Sketch of the geometric constraints (adapted from Ref. 16).

https://doi.org/10.1017/S0001924000008460 Published online by Cambridge University Press

or other celestial bodies, see Fig. 1(a). This is equivalent to guaranteeing that during the whole reorientation manoeuvre the following constraints are met: (1) the unit vector $\mathbf{n_P}$ remains outside m right circular cones generated around the forbidden directions, and (2) the unit vector $\mathbf{n_{SA}}$ lies inside a suitable right circular cone generated around the Sun-spacecraft direction. For instance, Fig. 1 shows the pointing constraints due to Sun, Earth, Moon and Jupiter. Undesired spacecraft orientations are expressed through mathematical inequalities in the form:

$$\delta_i \triangleq \text{Arccos}(\mathbf{n}_P \cdot \mathbf{n}_i) > \hat{\delta}_i \qquad \text{for } i = 1,\ldots,m \qquad \ldots (1)$$

whereas the constraint due to the solar array pointing requirement can be written as:

$$\gamma \triangleq \text{Arccos}(\mathbf{n}_{SA} \cdot \mathbf{n}_\odot) < \hat{\gamma} \qquad \ldots (2)$$

where $\hat{\gamma}$ is shown in Fig. (b).

Assume that the spacecraft has to align the scientific payload line-of-sight with a target direction (defined through the unit vector $\mathbf{n}_\star$) whose components are known in the inertial reference frame $\mathcal{T}_\text{I}$, see Fig. 1(b). The attitude control law must assure that the target direction is caught and maintained within specified limits. This amounts to stating that, at the end of the reorientation manoeuvre, both the final angle δ_f between the target direction and the scientific payload line-of-sight, and the modulus of the spacecraft's angular velocity $\|\boldsymbol{\omega}_f\|$ must be sufficiently small, i.e.:

$$\delta f \le \delta^{max} \text{ and } \|\boldsymbol{\omega} f\| \le \omega^{max} \qquad \ldots (3)$$

where δ is the angle between the directions of $\mathbf{n}_P$ and $\mathbf{n}_\star$, *viz*.

$$\delta \triangleq \text{Arccos}(\mathbf{n}_P \cdot \mathbf{n}_\star) \qquad \ldots (4)$$

In other terms, the problem consists of finding a suitable control law such that the target direction is reached within the prescribed requirements given by Equation (3), and the geometric constraints (1-2) are met along the whole spacecraft reorientation manoeuvre.

3.0 MATHEMATICAL MODEL

Consider a body axes reference frame $\mathcal{T}_B(x,y,z)$ with its origin in the spacecraft's centre-of-mass O, where x, y and z are the principal axes of inertia of the spacecraft and let ***i, j, k*** be the corresponding unit vectors. The unit quaternion is chosen to globally represent the spacecraft attitude without singularities[18]. Using the Euler's eigenaxis rotation theorem, the angular orientation of $\mathcal{T}_B$ relative to the inertial frame is expressed through the well known transformation matrix $\mathbf{T}$:

$$\mathbf{T} = \begin{bmatrix} q_0^2+q_1^2-q_2^2-q_3^2 & 2(q_1q_2-q_0q_3) & 2(q_0q_2+q_1q_3) \\ 2(q_1q_2+q_0q_3) & q_0^2-q_1^2+q_2^2-q_3^2 & 2(q_2q_3-q_0q_1) \\ 2(q_1q_3-q_0q_2) & 2(q_2q_3+q_0q_1) & q_0^2-q_1^2-q_2^2+q_3^2 \end{bmatrix} \qquad \ldots (5)$$

where $\boldsymbol{q} \triangleq (q_0, q_1, q_2, q_3)^T$ is the quaternion unit vector[6] associated with $\mathbf{T}$. In other terms, if $\boldsymbol{w}$ is an arbitrary vector, its components $(\mathbf{w})_{\mathcal{T}_B}$ expressed in the body axes reference frame are transformed from $\mathcal{T}_B$ to $\mathcal{T}_\text{I}$ through the equation:

https://doi.org/10.1017/S0001924000008460 Published online by Cambridge University Press

$$(\mathbf{w})_{TI} = \mathbf{T}(\mathbf{w})_{TB} \quad \ldots (6)$$

For the sake of simplicity, in the following the notation will be adopted. The Euler's rotational equations of motion for the (rigid) spacecraft, about its centre-of-mass O, are:

$$[\mathbf{M}] = \mathbf{I}[\boldsymbol{\omega}] + \Omega\mathbf{I}[\boldsymbol{\omega}] \quad \ldots (7)$$

with

$$\mathbb{I} \triangleq \begin{bmatrix} I_x & 0 & 0 \\ 0 & I_y & 0 \\ 0 & 0 & I_z \end{bmatrix} \quad ; \quad \Omega \triangleq \begin{bmatrix} 0 & -\omega_z & \omega_y \\ \omega_z & 0 & -\omega_x \\ -\omega_y & \omega_x & 0 \end{bmatrix} \quad \ldots (8)$$

whereas the kinematic equations of angular motion are:

$$[\dot{\mathbf{q}}] = \mathbf{E}[\boldsymbol{\omega}] \qquad \text{with} \qquad \mathbf{E} \triangleq \frac{1}{2}\begin{bmatrix} -q_1 & -q_2 & -q_3 \\ q_0 & -q_3 & q_2 \\ q_3 & q_0 & -q_1 \\ -q_2 & q_1 & q_0 \end{bmatrix} \quad \ldots (9)$$

In Equation (7), vector $[\mathbf{M}] \triangleq (M_x, M_y, M_z)^T$ is the total external moment about O, $[\omega] \triangleq (\omega_x, \omega_y, \omega_z)^T$ is the angular velocity of the spacecraft relative to T_I, whereas I_x, I_y and I_z are the vehicle's principal moments of inertia. In this paper the only external moments are given by the control system, the disturbance torques being negligible.

4.0 LYAPUNOV-BASED CONTROLLER

In the following we assume ideal thrusters, capable of generating independent continuous torques along the three principal axes in the range $(-M_i^{max}, M_i^{max})$ According to McInnes[13], a continuous control torque can be generated using pulse-width, pulse-frequency modulation of cold gas thrusters. As an alternative, the necessary continuous control torque can also be obtained with electric thrusters. However, in the latter case, a bank of thrusters is probably necessary. In fact, the maximum thrust of a single electric thruster suitable for attitude control usually does not exceed a few hundred millinewtons.

To introduce the control law, consider the state vector $\mathbf{x} \triangleq [\mathbf{q}^T, \boldsymbol{\omega}^T]^T$ and an artificial potential function, defined as:

$$V(\mathbf{x}) \triangleq V_\delta + V_\omega \quad \ldots (10)$$

where

$$V_\delta \triangleq \lambda_1 \frac{\delta^2}{2}\left(f_\gamma + \sum_{i=1}^{m} f_i \right) \quad \ldots (11)$$

$$V_\omega \triangleq \frac{1}{2\eta M^{\max}}[\boldsymbol{\omega}]^T \mathbf{I}[\boldsymbol{\omega}] \quad \ldots (12)$$

https://doi.org/10.1017/S0001924000008460 Published online by Cambridge University Press

and

$$f_\gamma = \begin{cases} \dfrac{1}{\lambda_2 + \left(\hat{\gamma} - \gamma\right)^2} & \text{if} \quad \gamma \le \hat{\gamma} \\ \gamma^2 / \left(\lambda_2 \hat{\gamma}^2\right) & \text{if} \quad \gamma > \hat{\gamma} \end{cases} \quad ; \quad f_i = \begin{cases} \dfrac{1}{\lambda_2 + \left(\delta_i - \hat{\delta}_i\right)^2} & \text{if} \quad \delta_i \ge \hat{\delta}_i \\ 2\hat{\delta}_i^2 / \left[\lambda_2 \left(\hat{\delta}_i^2 + \delta_i^2\right)\right] & \text{if} \quad \delta_i < \hat{\delta}_i \end{cases} \qquad \ldots (13)$$

In Equations (11)-(12), λ_1, λ_2 and η are dimensionless positive design parameters, and M^{max}(which is used to make V_ω dimensionless) is the maximum value of the control torques modulus, that is:

$$M^{\max} \triangleq \max\left\{ |\, M_x^{\max} \,|, |\, M_y^{\max} \,|, |\, M_z^{\max} \,| \right\} \qquad \ldots (14)$$

Note that both V_δ and V_ω are functions of the state vector **x**, because $\delta = \delta(\mathbf{q})$ via Equations (4,5 and 6). Also, $V(\boldsymbol{x}) > 0 \ \forall \boldsymbol{x} \neq \boldsymbol{x}_f$ ($\boldsymbol{x}_f$ is the target state) and $V(\boldsymbol{x}) \to \infty$ as $\|\boldsymbol{x}\| \to \infty$.

The artificial potential function is the sum of two terms: the first one (V_δ) depending on the spacecraft attitude (see Equation (11)) and, in particular, on the position of the scientific payload line-of-sight (δ) or the solar arrays (γ) with respect to the direction of the pointing constraints and of the target. The second (V_ω), instead, depends only on the rotational kinetic energy of spacecraft (see Equation (12)). Both potential functions and , being quadratic functions in δ and $\|\boldsymbol{\omega}\|$, always assume non-negative values and vanish only if $\delta = 0$ and $\|\boldsymbol{\omega}\| = 0$, that is, when the spacecraft angular velocity is zero and the scientific payload axis is aligned with the target direction.

The terms in Equation inversely proportional to the square of the angular distance between the scientific payload line-of-sight and the undesired space directions, create high potential regions. These latter, when used in conjunction with an appropriate control law, are able to guarantee that the constraints (1) and (2) are met along the whole spacecraft trajectory. In particular, the expressions of f_γ and f_i for $\gamma > \hat{\gamma}$ and $\delta_i < \hat{\delta}_i$ are introduced in Equation to push the state away from the forbidden region and avoid that a failure in the attitude control system causes the spacecraft to violate the geometric constraints[1,2].

Having defined the potential function V, it is now necessary to evaluate its time derivative. Bearing in mind Equations (10)-(12) and recalling Equation (9), the rate of change of is given by:

$$\dot{V} = [\boldsymbol{\omega}]^{\mathrm{T}} \mathbf{E}^{\mathrm{T}} \left(\nabla V_\delta\right)^{\mathrm{T}} + \frac{1}{\boldsymbol{\eta} M^{\max}} [\boldsymbol{\omega}]^{\mathrm{T}} \mathbf{I} [\dot{\boldsymbol{\omega}}] \qquad \ldots (15)$$

where:

$$\nabla V_\delta \triangleq \left[\frac{\partial V_\delta}{\partial q_0}, \frac{\partial V_\delta}{\partial q_1}, \frac{\partial V_\delta}{\partial q_2}, \frac{\partial V_\delta}{\partial q_3} \right]$$

A nonlinear control law can be developed to enforce the condition:

$$\dot{V} = -k [\boldsymbol{\omega}]^{\mathrm{T}} [\boldsymbol{\omega}] \qquad \ldots (16)$$

where $k > 0$ is a control gain to be chosen such that $\dot{V}$ is negative semi-definite. Note that $\dot{V} = 0$ implies that the spacecraft has reached the target condition (that is, $\delta = 0$ and $\|\boldsymbol{\omega}\| = 0$) or is at a saddle point. Although isolated saddle points may occur, usually these are unstable points[14] that cannot trap the system. Therefore, according to the global invariant set theorem[19], the spacecraft trajectory globally asymptotically converges to the desired (target) state.

https://doi.org/10.1017/S0001924000008460 Published online by Cambridge University Press

Extensive simulations have highlighted the presence of saddle points when the number of geometric constraints is moderate (typically two or three forbidden cones). For topologically complex regions, caused by the intersection of a number of forbidden conical constraints, overlapping potential barriers could be created in regions that are not filled by an actual physical constraint. In general this phenomenon tends to reduce (or even to prevent) the rate of convergence of spacecraft dynamics toward the target direction. However, this is usually a temporary problem because the space position of the forbidden cones varies with time.

Return now to the problem of autonomous reorienting manoeuvre and consider the control law

$$[\mathbf{M}] = -\boldsymbol{\eta} k M^{\max}[\boldsymbol{\omega}] - \boldsymbol{\eta} M^{\max} \mathbf{E}^{\mathrm{T}} (\nabla V_{\delta})^{\mathrm{T}} + \Omega \mathbf{I}[\boldsymbol{\omega}] \qquad \ldots (17)$$

Recalling Equation (7), the previous control law is shown to guarantee that $\dot{V}$ meets Equation (16) as long as no saturation occurs. In particular, the independent parameters η and k permit to tune the relative importance of the three terms in Equation . However, when the required control torques are outside the thruster operating range[14] (saturation condition), Equation (17) cannot be used, and is modified as[14]:

$$M_i = sign\left(M_i\right) M_i^{\max} \qquad \text{if} \qquad |M_i| > M_i^{\max} \quad \text{with} \quad i = \{x, y, z\} \qquad \ldots (18)$$

where sign (·) is the signum function. Because stability is not guaranteed in the presence of control saturation, extensive simulations are needed to validate the control law in a real mission scenario. In this case a different approach, which involves a backstepping technique, has been recently proposed[20] to reduce both the peak control torque and the reorientation time interval.

We are now in a position to better discuss the effect of λ_1 and λ_2 in Equation (11). The introduction of $\lambda_2 > 0$ implies that the potential function cannot take an infinite value and, at the same time, it is useful to shape the artificial potential slope. This is important because an eccessive value of the artificial potential slope would be unmanageable from the control law viewpoint. Indeed, as is shown by Equation (17), a high value of ∇V_{δ} implies a control torque that cannot be supplied by the attitude propulsion system, due to the thruster's operational constraints[18]. On the other hand, the parameter $\lambda_1 > 0$ allows one to scale the artificial potential function and to limit its maximum value. In fact, high potential values would cause unwanted overlapping phenomena, especially in the boundary regions around the undesired space orientations. This in turn would create space regions with high potential that would be almost unattainable by the spacecraft.

5.0 VARIABLE GAIN CONTROL

The characteristics of the spacecraft response, whose control law is described by Equations (17-18), are strongly dependent on the choice of the design parameter k. In particular, assuming that the torque level is within its operational range and substituting Equation (7) into (17), the spacecraft angular velocity may be expressed as:

$$[\boldsymbol{\omega}] + k\boldsymbol{\eta} M^{\max} \mathbf{I}^{-1}[\boldsymbol{\omega}] + \boldsymbol{\eta} M^{\max} \mathbf{I}^{-1} \mathbf{E}^{\mathrm{T}} \left(\nabla V_{\delta}\right)^{\mathrm{T}} = 0 \qquad \ldots (19)$$

Using a sufficiently high value of k, such that $k\,\eta\, M^{max}/I^{min} >> 1$ and $k\|\omega\| >> \|\mathbf{E}^{T} (\nabla V_{\delta})^{T}\|$ (where $I^{\min} \triangleq \min(I_x, I_y, I_z)$), Equation (19) is approximated by:

$$[\dot{\boldsymbol{\omega}}] + k\boldsymbol{\eta} M^{\max} \mathbf{I}^{-1}[\boldsymbol{\omega}] \approx 0 \qquad \ldots (20)$$

https://doi.org/10.1017/S0001924000008460 Published online by Cambridge University Press

The resulting dynamics is characterised by a fast angular velocity reduction. Indeed, the spacecraft's rotational motion is equivalent to that of a first order system with a small time constant. This behavior is well suited during the pointing terminal phase, when the payload line-of-sight is nearly aligned with the target direction (more precisely when $\delta < \delta_{th}$, where δ_{th} is a given threshold value of the slew angle), and the rotational velocity modulus is sufficiently small. In fact, in such a situation the angular velocity should be quickly set to zero in order to stop the spacecraft rotational motion at the desired target attitude.

It should be noted that a high value of k cannot be used when the scientific payload axis is far from the target direction, and the rotational velocity modulus is not sufficiently small, otherwise either a control input saturation occurs or an undesired slowing down of the spacecraft reorientation manoeuvre takes place. The reason is that when the angular velocity is high, such that the propulsion system torque is saturated, Equations (17) and (18) state that $\mathbf{M}$ is essentially in opposite direction with respect to $\boldsymbol{\omega}$. This characteristics tends to slow down the spacecraft rotational motion regardless of the value of δ (that is, the angular distance of payload axis from the target direction).

On the other hand, too small a value of k would cause the violation of the pointing constraints[1,2]. In fact, because the thruster torques cannot exceed a maximum value, the spacecraft must avoid approaching a pointing constraint with a high angular velocity, otherwise the control system would be unable to arrest the spacecraft before the constraint is violated. To further investigate this point it is useful to estimate the time interval $\mathcal{T}_i$ needed by the control system to set to zero the spacecraft angular velocity about its i-th principal axes (with $i = (x,y,z)$, starting from an initial angular velocity $\omega_{i0} \neq 0$.

The minimum time interval $\mathcal{T}_i$ is obtained when the absolute value of the control torque is at maximum, i.e., when $|M_i| = M_i^{max}$. In that case $\mathcal{T}_i = I_i \omega_{i0} / M_i^{max}$, see Sidi[21]. Correspondingly, the absolute value of the generic rotation angle $\Delta\theta_i$, which the spacecraft performs before the angular velocity modulus is zeroed, is given by:

$$\Delta\theta_i = -\frac{M_i^{\max} T_i^2}{2I_i} + \omega_{i_0} T_i = \frac{\omega_{i_0}^2 I_i}{2M_i^{\max}} \leq \frac{\omega_0^2 I^{\max}}{2M^{\min}} \qquad \ldots (21)$$

where $I^{max} \triangleq \max(I_x, I_y, I_z)$, $\boldsymbol{\omega}_0 \triangleq \|\omega(t_0)\|$, and $M^{min} \triangleq \min(M_x^{max}, M_y^{max}, M_z^{max})$. To avoid that during the slowing down manoeuvre the scientific payload axis may violate the pointing constraints, it is sufficient to enforce the condition:

$$\frac{\omega_0^2 I^{\max}}{2M^{\min}} \leq \delta^{\min} \triangleq \min\left\{|\,\delta_1 - \hat{\delta}_1\,|,\ldots,|\,\delta_m - \hat{\delta}_m\,|\right\}_{t=t_0} \qquad \ldots (22)$$

Dropping the dependence on t_0 (which is a generic time instant) the preceding equation provides an estimate of the maximum acceptable value of the actual spacecraft's angular velocity modulus $\omega = \|\boldsymbol{\omega}\|$ during the reorientation manoeuvre, *viz*.

$$\omega \leq \omega_{\max} \triangleq \sqrt{\frac{2M^{\min}\delta^{\min}}{I^{\max}}} \qquad \ldots (23)$$

In other terms, the spacecraft cannot exceed a certain angular velocity (or rotational kinetic energy) given by inequality[23], otherwise the control system is unable to safely arrest its manoeuvre when a geometric pointing constraint is going to be violated (note, however, that Equation (23) is a sufficient condition).

https://doi.org/10.1017/S0001924000008460 Published online by Cambridge University Press

The above considerations suggest using a variable control gain k whose instantaneous value depends both on the actual slew angle δ and on the spacecraft angular velocity modulus ω. More precisely, the suggested control law is as follows:

$$k = \begin{cases} k_h \ \text{ if } \ (\boldsymbol{\delta} < \boldsymbol{\delta}_{th}) \cup (\boldsymbol{\omega} \geq \sqrt{2M^{\min}\boldsymbol{\delta}^{\min}/I^{\max}}) \\ k_l \qquad\qquad\qquad otherwise \end{cases} \qquad \ldots (24)$$

where $k_h >> k_l$ is a high gain value that guarantees a sharp drop of spacecraft angular velocity near the target direction or a forbidden region. Of course, Equation (24) makes k to be time dependent. However, to simplify its practical implementation, the value of k may be updated only at constant time intervals of length Δt.

6.0 NUMERICAL SIMULATIONS

A large angle reorientation manoeuvre for a space telescope is now illustrated using the previous methodology. In particular, the geometric-inertial data of the Infrared Space Observatory (ISO) are considered[16,22], whose principal moments of inertia are $I_x = 6{,}587\text{kgm}^2$, $I_y = 7{,}526\text{kgm}^2$ and $I_z = 3{,}813\text{kgm}^2$. The control torques are assumed in the range $M_x \in (-2{\cdot}8, 2{\cdot}8)$ N m, whereas M_y and M_z are within (–3·6, 3·6) N m. These values are representative of thruster pairs mounted on the telescope periphery and capable of providing a maximum thrust of about 1N. These values are consistent with those discussed in Ref. 13.

Assume that $\boldsymbol{n}_P \equiv \boldsymbol{k}$ and $\boldsymbol{n}_{SA} \equiv \boldsymbol{i}$, and consider the pointing constraints due to Sun, Earth, Moon and Jupiter. Recalling Fig. 1 and Equation (1), the maximum solar array sun angle and the aperture of the forbidden cone are shown in Table 1. The latter also defines the gains of the control law,

Table 1
Geometric and control law data

parameter	value	units
k_h	1,000	
k_l	1	
$I^{\max}$	7,526	kgm^2
$M^{\max}$	3·6	Nm
$M^{\min}$	2·8	Nm
Δt	10	s
η	1	
λ_1	1	
λ_2	0·01	
$\hat{\gamma}$	30	deg (°)
δ_{th}	5	deg (°)
$\hat{\delta}_{\odot}$	27	deg (°)
$\hat{\delta}_{\oplus}$	65	deg (°)
$\hat{\delta}_{\leftmoon}$	24	deg (°)
$\hat{\delta}_{\odot}$	7	deg (°)

https://doi.org/10.1017/S0001924000008460 Published online by Cambridge University Press

such as k_h and k_l, which have been chosen with a trial and error procedure. A set of simulations are necessary to obtain a satisfactory result, because the control law performances are affected by the value of the selected gains. Note that the angular constraints for the reference spacecraft are compatible with the requirements of a typical infrared telescope[22].

A slewing rest-to-rest ($\omega_{x0} \equiv \omega_{y0} \equiv \omega_{z0} = 0$) manoeuvre of near 113° has been simulated, where the target is particularly difficult to be reached because its position is near the intersection of two forbidden cones (see Fig. 2). At the beginning of the reorientation manoeuvre, the components in the inertial reference frame $\mathcal{T}_I$ of the scientific payload axis $\boldsymbol{n}_P$, the forbidden directions, and the target position $n_\star$ are:

$$[\mathbf{n}_P]_{\mathcal{T}_I} = \begin{bmatrix} 0 \\ 0 \\ 1 \end{bmatrix} \quad , \quad [\mathbf{n}_\odot]_{\mathcal{T}_I} = \begin{bmatrix} 1 \\ 0 \\ 0 \end{bmatrix} \quad , \quad [\mathbf{n}_\leftmoon]_{\mathcal{T}_I} = -0{\cdot}5 \begin{bmatrix} 1 \\ \sqrt{3} \\ 0 \end{bmatrix} \qquad \ldots \ (25)$$

$$[\mathbf{n}_\oplus]_{\mathcal{T}_I} = 0{\cdot}5 \begin{bmatrix} 1 \\ \sqrt{3} \\ 0 \end{bmatrix} \quad , \quad [\mathbf{n}_\circledcirc]_{\mathcal{T}_I} = \begin{bmatrix} 0 \\ 1 \\ 0 \end{bmatrix} \quad , \quad [\mathbf{n}_\star]_{\mathcal{T}_I} = -\begin{bmatrix} 0{\cdot}0958 \\ 0{\cdot}8962 \\ 0{\cdot}433 \end{bmatrix} \qquad \ldots \ (26)$$

Since the unit vectors $\boldsymbol{n}_\mathrm{p}$ and $\boldsymbol{n}_\mathrm{SA}$ are assumed to be orthogonal, the solar array cones drawn in Fig. 2 are the auxiliary cones generated around the Sun-spacecraft direction with semi-aperture angles equal to $\beta \triangleq (90° - \hat{\gamma})$ These are useful to visualise the exclusion cones for the payload pointing direction associated with the solar array cone within which the vector $\boldsymbol{n}_\mathrm{SA}$ is constrained

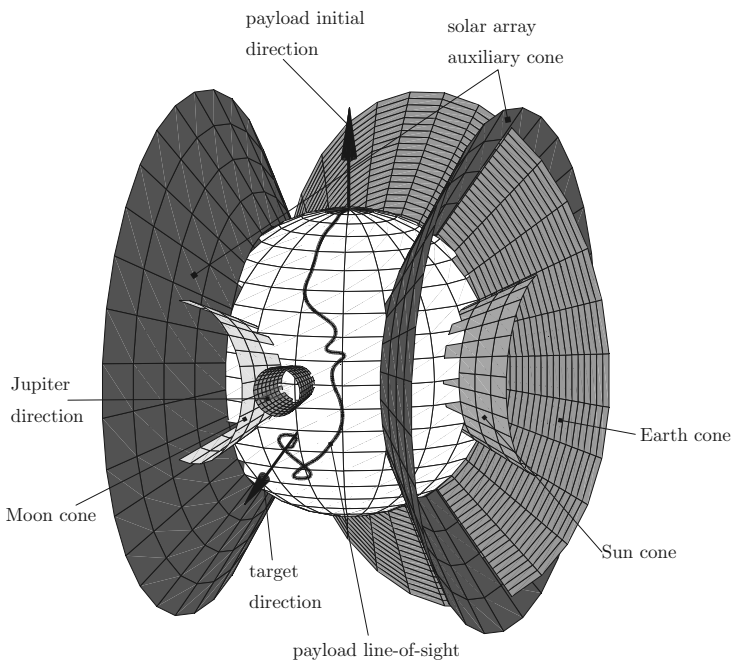


Figure 2. Sketch of the spacecraft reorientation manoeuvre with the payload initial direction, the target direction and the visible constraints.

https://doi.org/10.1017/S0001924000008460 Published online by Cambridge University Press

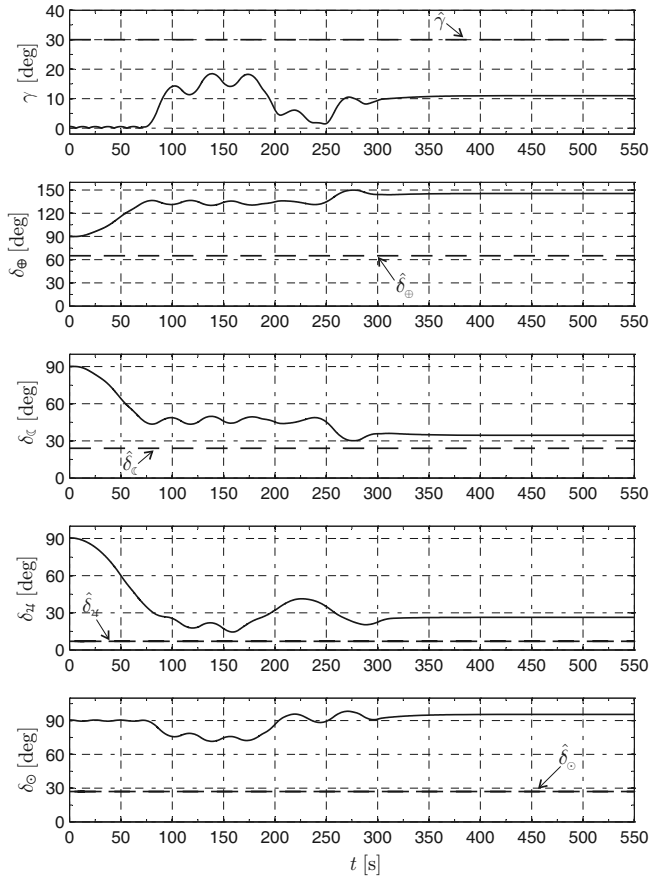


Figure 3. Time variation of angles γ, $\delta_{\oplus}$, $\delta_{\leftmoon}$, $\delta_{\odot}$, and $\delta_{\odot}$ during the slew manoeuvre.

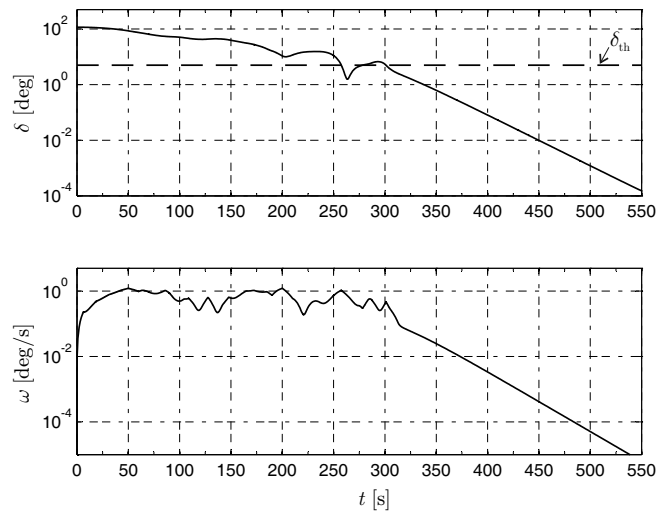


Figure 4. Semi-logarithmic plots of slew angle and spacecraft angular velocity as a function of time.

https://doi.org/10.1017/S0001924000008460 Published online by Cambridge University Press

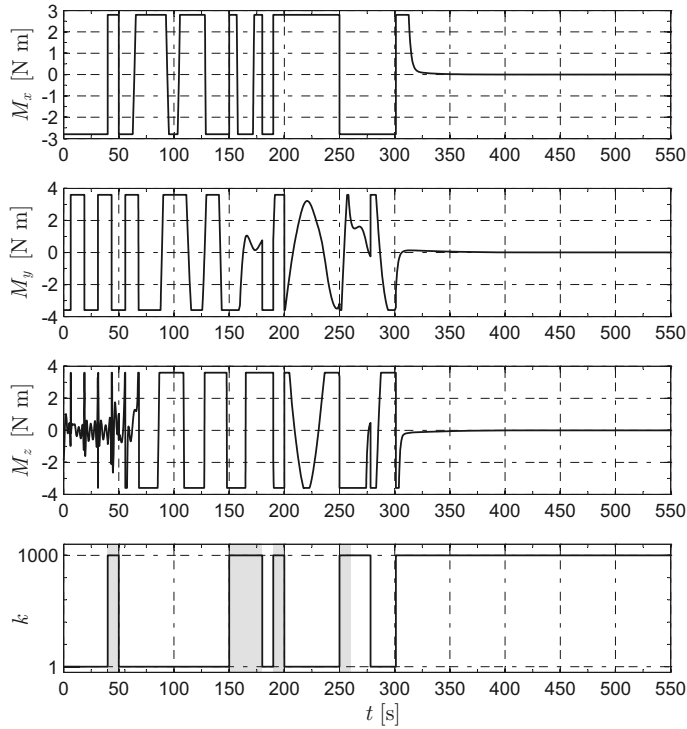


Figure 5. Time histories of control torques M_x, M_y and M_z , and the control gain k.

to lie. Figure 2 also shows the payload line-of-sight time history. It is clear that all the constraints are met along the spacecraft reorientation trajectory. The effectiveness of the control system is better appreciated with the aid of Fig. 3, where the plots of $\delta_{\oplus}$, $\delta_{\leftmoon}$, $\delta_{\odot}$, and $\delta_{\odot}$ show that they keep above the specified minimum values.

Figure 4 illustrates the slew angle δ and the modulus of the spacecraft angular velocity It should be noted that, at the end of the manoeuvre, both constraints are met. In particular the slew angle becomes smaller than 1×10^{-2}deg in about 450s.

Figure 5 shows the variations of the control gain k with time as well as the time histories of the components of the control torque $\boldsymbol{M}$ in the body reference frame $\mathcal{T}_B$. In particular, the grey zones in the time history of k have been added to highlight the time intervals within which $\omega > \omega_{max}$, see Equation (23). During these time intervals k is at maximum (recall Equation (24)), the command torque is saturated and the spacecraft tends to decelerate the rotational motion see Fig. 4.

Note the final increase of k that occurs when the slew angle achieves the threshold value δ_{th}, see Fig. 4. In this situation the spacecraft quickly sets to zero its angular velocity following a first-order dynamics, in accordance with Equation (20). Also note that a saturation exists in all of the control torque components.

7.0 CONCLUSIONS

A new methodology has been developed to handle large angle slew manoeuvres with pointing constraints. The problem of attitude control has been formulated and solved through artificial

https://doi.org/10.1017/S0001924000008460 Published online by Cambridge University Press

potential functions, thus considerably simplifying the spacecraft reorientation manoeuvres with autonomous re-targeting capabilities. Unlike the usual approaches available in the literature, a time variant control gain is chosen to reduce the duration of the reorientation manoeuvre. The rationale is that high values of the control gain correspond to a slow spacecraft movement, whereas small values of k give rise to rapid reorientation manoeuvres. The control gain value depends both on the system kinetic energy and on the distance of the spacecraft from the target direction. As a result, close connections between the control law and fundamental physical quantities are established. More important, the spacecraft is able to reach points in the potential field arbitrarily close to a constraint and to manoeuvre with autonomous capability of guidance and control. Accordingly, autonomous avoidance of undesired space orientations is obtained and constraints due to the solar array pointing requirements are met.

REFERENCES

1. KUMAR, R.R. Artificial Neural Networks in Space Station Optimal Attitude Control, World Space Congress, Washington DC, USA, 27 August – 4 September 1992, Paper IAF-92-0038.
2. FRAKES, J.P., HENRETTY, D.A., FLATLEY, T.W., MARKLEY, L.F., SAN, J.K. and LIGHTSEY, E.G. SAMPEX Science Pointing with Velocity Avoidance, AAS/AIAA Spaceflight Mechanics Meeting, Colorado Springs, CO, USA, 24–26 February 1992, Paper AAS 92-182.
3. SINGH, G., MACALA, G., WONG, E.C. and RASMUSSEN, R.D. A Constraint Monitor Algorithm for the Cassini Spacecraft, AIAA Guidance, Navigation, and Control Conference, New Orleans, LA, USA, August 1997, Paper AIAA 97-3526.
4. SØRENSON, A.M. ISO Attitude manoeuvre strategies, *Advances in the Astronautical Sciences,* **84**, 1993, pp 975–987.
5. WIE, B. and BARBA, P.M. Quaternion feedback for spacecraft large angle manoeuvres, *J Guidance, Control, and Dynamics*, May-June 1985, **8**, (3), pp 360–365. doi: 10.2514/3.19988.
6. BILIMORIA, K.D. and WIE, B. Time-optimal three-axis reorientation of a rigid spacecraft, *J Guidance, Control and Dynamics*, May-June 1993, **16**, (3), pp 446–452. doi: 10.2514/3.21030.
7. SHEN, H. and TSIOTRAS, P. Time-optimal control of axisymmetric rigid spacecraft using two controls, *J Guidance, Control, and Dynamics*, September-October 1999, **22**, (5), pp 682–694. doi: 10.2514/2.4436.
8. LIU, S.W. and SINGH, T. Fuel/time optimal control of spacecraft manoeuvres, *J Guidance, Control, and Dynamics*, March-April 1997, **20**, (2), pp 394–397. doi: 10.2514/2.4053.
9. BRYSON, A.E. and HO, Y.C. *Applied Optimal Control*, chap 2, Hemisphere Publishing Corporation, New York, NY, 1975, pp 117–125, ISBN: 0-891-16228-3.
10. MELTON, R.G. Hybrid Methods for Determining Time-Optimal, Constrained Spacecraft Reorientation Manoeuvres, IAA Conference on Dynamics and Control of Space Systems, Porto, Portugal, March 2012, Paper IAA-AAS-DyCoSS1-07-08.
11. MELTON, R.G. Numerical analysis of constrained, time-optimal satellite reorientation, *Mathematical Problems in Engineering*, 2012, pp 1–19, Article ID 769376. doi: 10.1155/2012/769376.
12. MCINNES, C.R. Potential Function Methods for Autonomous Spacecraft Guidance and Control, AAS/AIAA Astrodynamics Specialist Conference, Halifax, Nova Scotia, Canada, August 1995, Paper AAS 95-447.
13 MCINNES, C.R. Large angle slew manoeuvres with autonomous sun vector avoidance, *J Guidance, Control and Dynamics*, July-August 1994, **17**, (4), pp 875–877. doi: 10.2514/3.21283.
14. RADICE, G. and MCINNES, C.R. Constrained on-board attitude control using gas jet thrusters, *Aeronaut J*, December 1999, **103**, (1030), pp 549–556.
15. CASASCO, M. and RADICE, G. Autonomous slew manoeuvring and attitude control using the potential function method, *Advances in the Astronautical Sciences*, 2003, **116**, pp1745-1765.
16. MENGALI, G. and QUARTA, A.A. Spacecraft control with constrained fast reorientation and accurate pointing, *Aeronaut J*, February 2004, **108**, (1080), pp 85–91.
17. HABLANI, H.B. Attitude commands avoiding bright objects and maintaining communication with ground station, *J Guidance, Control, and Dynamics*, November-December 1999, **22**, (6), pp 759-767. doi: 10.2514/2.4469.

https://doi.org/10.1017/S0001924000008460 Published online by Cambridge University Press

18. MEYER, G. Design and Global Analysis of Spacecraft Attitude Control Systems, Tech rep, NASA, March, **1**, 1971, NASA TR-R-361.
19. SLOTINE, J.-J. E. and LI, W. *Applied Nonlinear Control*, Prentice Hall, Englewood Cliffs, NJ, USA, 1991, pp 73–74, ISBN: 0-130-40890-5.
20. ALI, I., RADICE, G. and KIM, J. Backstepping Control Design with Actuator Torque Bound for Spacecraft Attitude Manoeuvre, *J Guidance, Control and Dynamics*, January-February 2010, **33**, (1), pp 254–259. doi: 10.2514/1.45541.
21. SIDI, M.J. *Spacecraft Dynamics and Control: A Practical Engineering Approach*, Cambridge University Press, New York, NY, USA, 1997, pp 140–141, ISBN: 0-521-78780-7.
22. LEECH, K. and POLLOCK, A.M.T. ISO – The Satellite and its Data, Vol **II** SAI/99-082/Dc, Space Science Department of ESA, Villafranca, PO Box 50727, E-28080 Madrid, Spain, July 2000, Version 1.0.

https://doi.org/10.1017/S0001924000008460 Published online by Cambridge University Press